AJNR

Correlation of MRI-Derived Apparent Diffusion Coefficients in Newly Diagnosed Gliomas with [^{18}F]-Fluoro-L-Dopa PET: What Are We Really Measuring with Minimum ADC?

S. Rose, M. Fay, P. Thomas, P. Bourgeat, N. Dowson, O. Salvado, Y. Gal, A. Coulthard and S. Crozier

AJNR Am J Neuroradiol 2013, 34 (4) 758-764
doi: https://doi.org/10.3174/ajnr.A3315
http://www.ajnr.org/content/34/4/758

Correlation of MRI-Derived Apparent Diffusion Coefficients in Newly Diagnosed Gliomas with [^{18}F]-Fluoro-L-Dopa PET: What Are We Really Measuring with Minimum ADC?

S. Rose, M. Fay, P. Thomas, P. Bourgeat, N. Dowson, O. Salvado, Y. Gal, A. Coulthard, and S. Crozier

ABSTRACT

BACKGROUND AND PURPOSE: There is significant interest in whether diffusion-weighted MR imaging indices, such as the minimum apparent diffusion coefficient, may be useful clinically for preoperative tumor grading and treatment planning. To help establish the pathologic correlate of minimum ADC, we undertook a study investigating the relationship between minimum ADC and maximum FDOPA PET uptake in patients with newly diagnosed glioblastoma multiforme.

MATERIALS AND METHODS: MR imaging and FDOPA PET data were acquired preoperatively from 15 patients who were subsequently diagnosed with high-grade brain tumor (WHO grade III or IV) by histopathologic analysis. ADC and SUVR normalized FDOPA PET maps were registered to the corresponding CE MR imaging. Regions of minimum ADC within the FDOPA-defined tumor volume were anatomically correlated with areas of maximum FDOPA SUVR uptake.

RESULTS: Minimal anatomic overlap was found between regions exhibiting minimum ADC (a putative marker of tumor cellularity) and maximum FDOPA SUVR uptake (a marker of tumor infiltration and proliferation). FDOPA SUVR measures for tumoral regions exhibiting minimum ADC (1.36 $\pm$ 0.22) were significantly reduced compared with those with maximum FDOPA uptake (2.45 $\pm$ 0.88, $P = .0001$).

CONCLUSIONS: There was a poor correlation between minimum ADC and the most viable/aggressive component of high-grade gliomas. This study suggests that other factors, such as tissue compression and ischemia, may be contributing to restricted diffusion in GBM. Caution should be exercised in the clinical use of minimum ADC as a marker of tumor grade and the use of this index for guiding tumor biopsies preoperatively.

ABBREVIATIONS: CE = contrast-enhanced; FDOPA = 3,4-dihydroxy-6-[^{18}F]-fluoro-L-phenylalanine; GBM= glioblastoma multiforme; SUVR = standardized uptake value ratio; WHO = World Health Organization

Despite the recent advances in neurosurgical resection techniques and adjuvant therapies, the median survival for patients diagnosed with glioblastoma multiforme remains poor at <15 months.[1] This devastating outcome can be attributed to 2 major factors: 1) the limitation of currently used diagnostic imaging, in particular MR imaging technology, to provide clinically relevant information about tumor proliferation and physiology; and 2) the failure of current therapies for targeting extremely invasive proliferating tumor cells, in many cases anatomically isolated from the main tumor mass. Routine contrast-enhanced MR imaging plays a pivotal role in the planning of treatment strategies. However, CE MR imaging only detects dysfunction of the blood-brain barrier, which, in many cases, may not correspond with tumor proliferation or other molecular events.[2] Many of these limitations have been overcome by using PET molecular imaging technology with amino acid–based tumor cell tracers, such as methyl-^{11}C-L-methionine[3] and 3,4-dihydroxy-6-[^{18}F]-fluoro-L-phenylalanine.[4,5] Such tracers have been shown to be superior in the diagnostic assessment of patients with brain tumor compared with CE MR imaging and 2-deoxy-2-[^{18}F]fluorodeoxyglucose PET.[4,6]

Due to the invasiveness and logistic constraints associated with routine clinical PET imaging, significant interest has been directed toward the clinical development of diffusion-weighted

Received February 21, 20102; accepted after revision July 6.

From the Centre for Clinical Research (S.R.), Centre for Medical Diagnostic Technologies in Queensland (Y.G., S.C.), and Discipline of Medical Imaging (A.C.), University of Queensland, St Lucia, Brisbane, Australia; and Department of Radiation Oncology (M.F.), Queensland PET Service (P.T.), Australian e-Health Research Centre (P.B., O.S., S.R.), Commonwealth Scientific and Industrial Research Organization; and Department of Medical Imaging (A.C.), Royal Brisbane and Women's Hospital, Herston, Brisbane, Australia.

This work was funded by the National Health and Medical Research Council (grant 631567) and a Queensland Government National and International Alliances Research Program grant.

Please address correspondence to Stephen Rose, PhD, Centre for Clinical Research, Royal Brisbane and Women's Hospital, Brisbane 4029, Australia; e-mail: Stephen.Rose@cai.uq.edu.au

http://dx.doi.org/10.3174/ajnr.A3315

MR imaging indices, such as the apparent diffusion coefficient, for preoperative tumor grading and treatment planning.[7] Because ADC provides quantitative information about tumor physiology on a macroscopic scale, the technique shows promise for aiding image-guided therapy, especially within biologically heterogeneous tumors such as GBM. However, the clinical utility of the technique for assessing tumor grade has yet to be established. Numerous studies have reported mixed findings regarding the use of ADC to measure tumor grade.[8-11] The rationale behind the use of ADC indices is based on the premise that tumor cellularity is inversely related to the ADC (ie, tumoral regions with low, sometimes termed "minimum," ADC correspond to areas of high cellularity).[7] One study has shown a significant correlation between minimum ADC and a measure of proliferation index (Ki–67) for astrocytic tumors in general; however, this correlation was not significant for GBM alone.[12] Because no study has yet performed minimum ADC–image-guided biopsy for histologic confirmation, this assumption remains highly speculative. Despite this constraint, a significant correlation has been established between the minimum ADC and reduced patient survival.[9,13]

A recent study aimed at investigating the relationship between minimum ADC and FDG-PET reported correlations between regions of low ADC and enhanced FDG uptake in patients with GBM.[13] However, the clinical interpretation of FDG uptake in primary brain tumors is complex due to high background glucose metabolism, especially within the cortex, and false-positive uptake associated with inflammatory and granulomatous disease.[14] To help establish the pathologic correlate of minimum ADC, we undertook a preliminary study investigating the relationship between minimum ADC and FDOPA PET uptake in patients with newly diagnosed GBM. Recent studies have shown that FDOPA has similar tumor uptake compared with methyl-^{11}C-L-methionine, resulting in a significant improvement in diagnostic accuracy compared with FDG-PET in evaluating both low- and high-grade tumors.[4,15] Furthermore the kinetic modeling of FDOPA uptake has been shown to be useful for establishing tumor grade[16] and has recently been shown to correlate with tumor Ki-67 proliferation indices in newly diagnosed gliomas.[17] Our underlying hypothesis is that if minimum ADC corresponds to regions of high tumor cellularity, then tumoral regions of low ADC should overlap considerably areas of high FDOPA uptake.

MATERIALS AND METHODS

The institutional review board approved the study and written informed consent was obtained from each participant.

Patients

Data from 15 patients (10 men; age range, 47–85 years) with histopathologically confirmed high-grade brain tumor (WHO grade III or IV) were used in this study. These patients were enrolled in a larger study aimed at developing FDOPA PET–MR imaging fusion-guided therapy for patients with primary brain tumors.

Imaging Protocols

Both the MR imaging and FDOPA PET studies were performed within 48 hours before tumor resection. MR imaging scans were performed by using a 3T Tim Trio scanner (Siemens, Erlangen, Germany). Routine diagnostic scans were supplemented with standard T1-weighted MR imaging scans (1-mm isotropic resolution) acquired before and after administration of contrast agent (0.1 mmol/kg of body weight, gadodiamide; Amersham Health, Oslo, Norway). Diffusion images were acquired by using high-angular-resolution diffusion imaging with the following parameters: 60 axial sections; FOV, 30 × 30 cm; TR/TE, 9200/112 ms; 2.5-mm section thickness; acquisition matrix, 128 × 128 with a 2.3 mm in-plane image resolution; acceleration factor of 2; and maximum diffusion-encoding gradient strength of $b = 3000$ s/mm^{-2}.

Sixty-five diffusion-weighted images were acquired at each location consisting of 1 low- ($b = 0$) and 64 high-diffusion-weighted images. The acquisition time for the diffusion dataset was 9.67 minutes. A field map for the diffusion data was acquired by using two 3D gradient recalled-echo images (TE1/TE2, 4.76/7.22 ms) to assist the correction for distortion due to susceptibility-induced inhomogeneity. This acquisition protocol was selected to enable the study of tumor infiltration along white matter tracts by using tractography-based analysis techniques. FDOPA preparation took place in a radiochemistry laboratory by using a previously reported synthesis.[18] PET imaging was performed by using a Gemini GXL scanner (Philips, Best, the Netherlands). An FDOPA activity of 151 MBq on average was administered intravenously (range, 138–164 MBq). A low-dose transmission CT scan was performed followed by a 75-minute list mode acquisition. The images were reconstructed by using ordered subset expectation maximization,[19] with corrections for attenuation and scatter.[20] The final volume had a matrix size of 128 × 128, consisting of 90 planes of 2 × 2 × 2 mm^3 voxels.

Diffusion Processing

To reduce image distortions and artifacts generated from involuntary head motion and physiologic noise, we used the following diffusion MR imaging preprocessing pipeline that has been fully described elsewhere.[21] In brief, raw diffusion-weighted images were corrected for subject motion by using the method described by Bai and Alexander.[22] Thus, the diffusion tensor was calculated from the (uncorrected) diffusion data. With the diffusion tensor information, a synthetic image was generated for every volume of the diffusion series. Every volume of the raw diffusion data was then aligned with the corresponding synthetic volume by using a 6-*df* registration performed with Advanced Normalization Tools (http://picsl.upenn.edu/ANTS), with the appropriate adjustment of the b-matrix.[23] Susceptibility distortions were corrected by using the field map with FUGUE and Phase Region Expanding Labeler for Unwrapping Discrete Estimates in raw image space, both part of fMRI of the Brain Software Library (FSL; http://www.fmrib.ox.ac.uk/fsl/), with signal-intensity correction. Motion artifacts were identified and replaced by using the detection and replacement of outliers before resampling method[24] in conjunction with the registration method by Bai and Alexander described above. ADC maps were then generated by using standard tools found within the MRtrix package (http://www.brain.org.au/software).[25]

Table 1: Patient demographics, minimum ADC, and maximum FDOPA measures

Patient	Sex/Age (yr)	Pathology	ADC Value[a]			FDOPA Value[a]	
			Normal Tissue	Min ADC ROI	Max FDOPA ROI	Min ADC ROI	Max FDOPA ROI
1	M/72	GBM	550 (30)	380 (50)	550 (130)	1.42 (0.402)	1.96 (0.18)
2	M/58	GBM	530 (28)	410 (30)	670 (70)	1.32 (0.36)	2.68 (0.22)
3	F/56	GBM	550 (25)	380 (90)	750 (170)	1.10 (0.34)	2.27 (0.19)
4	M/69	GBM	540 (28)	440 (10)	920 (170)	1.12 (0.13)	2.23 (0.33)
5	M/61	GBM	540 (30)	420 (30)	770 (130)	1.20 (0.13)	2.18 (0.21)
6	F/69	GBM	520 (25)	390 (60)	640 (80)	1.79 (0.69)	3.85 (0.36)
7	M/69	GBM	520 (30)	390 (60)	710 (140)	1.49 (0.21)	2.00 (0.22)
8	F/54	GBM	520 (30)	370 (11)	670 (140)	1.72 (0.62)	2.26 (0.36)
9	M/62	GBM	540 (25)	420 (40)	1170 (310)	1.21 (0.49)	5.01 (1.20)
10	F/47	AA	530 (30)	420 (20)	660 (190)	1.47 (0.20)	1.65 (0.18)
11	F/59	GBM	510 (30)	440 (20)	840 (130)	1.09 (0.26)	1.90 (0.22)
12	M/64	GBM	520 (30)	380 (50)	710 (110)	1.55 (0.38)	2.74 (0.34)
13	M/78	GBM	530 (34)	432 (39)	725 (165)	1.17 (0.25)	1.95 (0.17)
14	M/52	GBM	514 (40)	442 (27)	675 (162)	1.34 (0.18)	1.88 (0.23)
15	M/85	GBM	561 (30)	417 (35)	845 (167)	1.44 (0.26)	2.11 (0.28)
mean (SD)			531 (29)	409 (38)	790 (151)	1.36 (0.22)	2.45 (0.88)

Note:—Min indicates minimum; Max, maximum; AA, anaplastic astrocytoma.
[a] $\times 10^{-6}$ mm^2/s; mean (SD) ADC and FDOPA values are given for each patient including for the entire cohort.

FDOPA PET Processing and ADC Image Fusion

The FDOPA images were rigidly registered to the CE MR imaging by using a block matching approach with 6 *df*.[26] Normalization of the FDOPA scans was then performed by using the standardized uptake value ratio method, whereby each voxel was divided by the mean uptake in the cerebellum, a region that shows only nonspecific tracer uptake.[4] The cerebellum was manually defined on the FDOPA maps. To register the FDOPA and ADC maps, we rigidly aligned $b = 0$ images acquired as part of the High Angular Resolution Diffusion Imaging sequence to the coregistered CE MR imaging, by using the FSL Linear Image Registration Tool and 6 *df*, using mutual information.

Generation of Minimum ADC and Maximum FDOPA SUVR Regions

There is no widely accepted method to delineate tumor margins on the basis of FDOPA threshold levels, though the use of the percentage of maximum SUVR based on the tumor background ratio has been suggested.[27] Techniques based on the use of a single global threshold are not suitable for FDOPA images due to possible uptake within noncancerous tissue (striatum) close to the tumor and inhomogeneous tracer uptake within the whole tumor volume. In this study, an experienced nuclear medicine physician (P.T.) manually defined the tumor boundary by using the fused CE MR imaging and FDOPA maps. Regions of interest on the ADC maps, outside of the FDOPA-defined tumor volume, were manually placed to identify ADC measures in normal tissue. This placement was performed, when possible, on several serial axial sections containing no FDOPA uptake (ie, infiltrating tumor). Reference to coregistered CE MR imaging and T2-weighted scans was also considered to avoid including tissue exhibiting significant compression effects due to excessive tumor growth. The mean (SD) volume of normal tissue was 172 ± 54 mL. Regions of minimum ADC within the FDOPA-defined tumor volume were generated by applying a threshold of 450×10^{-6} mm^2/s (ie, 3 SDs lower than the mean ADC values derived for normal parenchymal tissue). Regions of maximum FDOPA uptake within the tumor volume were defined by voxels with the 20% highest SUVR.[17] Mean FDOPA SUVR indices were generated for the tumoral regions exhibiting minimum ADC. Mean ADC values within regions corresponding to maximum FDOPA SUVR were also calculated.

To evaluate the voxelwise anatomic relationship between these regions, binary threshold maps defining minimum ADC and maximum FDOPA SUVR regions were multiplied to generate an overlap map. The volume of this overlapping region was expressed as a percentage of the minimum ADC and maximum FDOPA tumor volumes. Significant differences between mean ADC and FDOPA indices were determined by using a Mann-Whitney *U* test (Statistical Package for the Social Sciences software, Version 19; SPSS, Chicago, Illinois).

RESULTS

Patient demographics and minimum ADC and maximum FDOPA values are shown in Table 1. Maximum FDOPA SUVR and minimum ADC-defined tumor volumes along with the percentage of region overlap are shown in Table 2. Box-and-whisker plots highlighting the differences in ADC and FDOPA SUVR measures for these regions are given in Fig 1. There was a considerable range in minimum ADC volume across the patient cohort (range, 0.3–29 mL). The maximum FDOPA SUVR tumor volumes were significantly larger than the corresponding minimum ADC defined volumes ($P = .0009$). With regard to diffusivity measures, the ADC values for the maximum FDOPA SUVR-defined tumor volumes ($790 \pm 151 \times 10^{-6}$ mm^2/s) were significantly higher compared with the minimum ADC defined volumes ($409 \pm 38 \times 10^{-6}$ mm^2/s; $P = .0007$). In addition, the ADC values for the maximum FDOPA SUVR tumor volumes were significantly higher compared with those measured in normal tissue ($531 \pm 29 \times 10^{-6}$ mm^2/s; $P = .0009$). FDOPA uptake within the maximum FDOPA SUVR-defined tumor volume (2.45 ± 0.88) was significantly higher than that found within the minimum ADC-defined tumor volume (1.36 ± 0.22, $P = .0012$). Most important, with regard to overlap between these 2 regions, most patients presented with no or only modest overlap. As highlighted

Table 2: Tumor volumetric measures

Patient	Max FDOPA Volume (mL)	Min ADC Volume (mL)	Overlap (%)[a]	Overlap (%)[b]
1	29.9	29.0	19.3	19.9
2	38.3	0.4	0.2	19.2
3	15.7	4.8	0.2	0.7
4	19.9	0.3	0	0
5	3.1	1.6	0	0
6	18.9	4.6	1.0	4.1
7	12.9	0.4	0.2	6.5
8	33.9	0.9	0.3	11.3
9	21.6	2.3	3.0	28.2
10	60.1	15.0	6.8	27.3
11	44.5	0.5	0	0
12	14.1	2.9	0.52	2.5
13	15.8	3.7	0.42	1.8
14	20.0	0.4	0.2	9.3
15	59.7	1.9	0.4	13.4

Note:—Min indicates minimum; Max, maximum.
[a] Overlap (ie, minimum ADC volume overlap with maximum FDOPA SUVR) expressed as a percentage of maximum FDOPA SUVR volume.
[b] Overlap (ie, minimum ADC volume overlap with maximum FDOPA SUVR) expressed as a percentage of mininum ADC volume.

in Table 2, the extent of minimum ADC volume with maximum FDOPA SUVR was, at most, 28%, based on the volume of the smallest region, namely the minimum ADC volume. Representative CE MR imaging, ADC, and FDOPA PET maps for patients with large minimum ADC volumes are given in Fig 2.

DISCUSSION

The major finding from this study was the limited anatomic overlap between tumor regions of minimum ADC and areas exhibiting maximum FDOPA SUVR. This result provides evidence that enhanced tumor cellularity may not be the key factor contributing to the restriction of water diffusion in GBM. Such a finding has significant clinical impact because measures of minimum ADC or differences between minimum and maximum ADC have been reported as potential markers of tumor grade,[8,9,12] albeit with conflicting views in the literature.[10,11,28] In addition, although many glioblastomas present with diverse heterogeneous patterns of diffusivity, most do not exhibit large regions of restricted diffusion.[28] In our preliminary study, 13 patients (approximately 86%) had minimum ADC regions of <5 mL in volume. However, we used a stringent ADC threshold level (450×10^{-6} mm/s^2), and selection of a higher ADC value would increase the minimum ADC volume. Because the aim of this study was to investigate the anatomic relationship between areas of minimum ADC (ie, proposed regions of high tumor cellularity) with areas of high FDOPA uptake, reducing this threshold would impact the interpretation of the findings because larger minimum ADC volumes would most likely contain tissue with varying degrees of tumor infiltration. We selected this threshold level because it falls 3 SDs below the mean ADC derived from normal tissue ($531 \pm 29 \times 10^{-6}$ mm/s^2) and provides a robust strategy for delineating minimum ADC volumes.

The rationale behind the use of ADC indices is based on the premise that increased tumor cellularity leads to an increase in volume of the intracellular space, which results in restricted water diffusion within the reduced extracellular compartment.[7] This concept is supported by the finding that some highly cellular tumors such as lymphomas also exhibit restricted diffusion.[29] However, a study investigating the relationship between minimum ADC and Ki-67 measures, a histologically-based tumor proliferation index, reported no significant correlation in patients with GBM.[12]

Most interesting, a recent study focusing on investigating the relationship between ADC and dynamic contrast-enhanced MR imaging measures of the volume of the extravascular extracellular space per unit volume (v_e) in patients with newly diagnosed gliomas reported that no correlation was found between ADC and v_e.[30] This study provides additional evidence that tumor regions with reduced diffusion do not necessarily correlate with tissue possessing a reduced extracellular compartment, and it highlights the belief that further work is required to establish the link between minimum ADC and tumor cellularity in newly diagnosed GBM. Despite the lack of imaging and histologic support for the this concept, a number of studies have shown a significant correlation between minimum ADC and reduced patient survival.[9,13]

Understanding ADC measures in primary brain tumors presents a significant challenge because high-grade gliomas contain a continuum of evolving histologic features (WHO classification grades II-IV), with the degree of water diffusivity related to a number of factors such as cellularity, edema, and degenerative changes associated with hemorrhage and cystic or mucinous degeneration along with compression effects within peritumoral tissue. Serial preoperative studies in patients[31] and animal models[32] have shown that diffusivity measures are continually evolving,

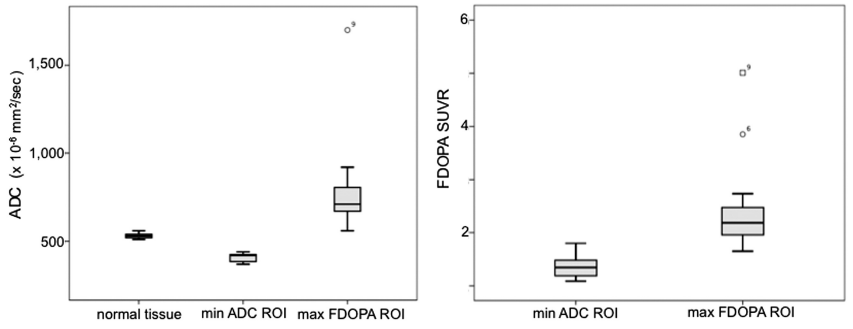

FIG 1. Box-and-whisker plots outlining the distribution (mean and SD) of ADC and FDOPA SUVR measures within the minimum ADC and maximum FDOPA SUVR–defined tumor regions.

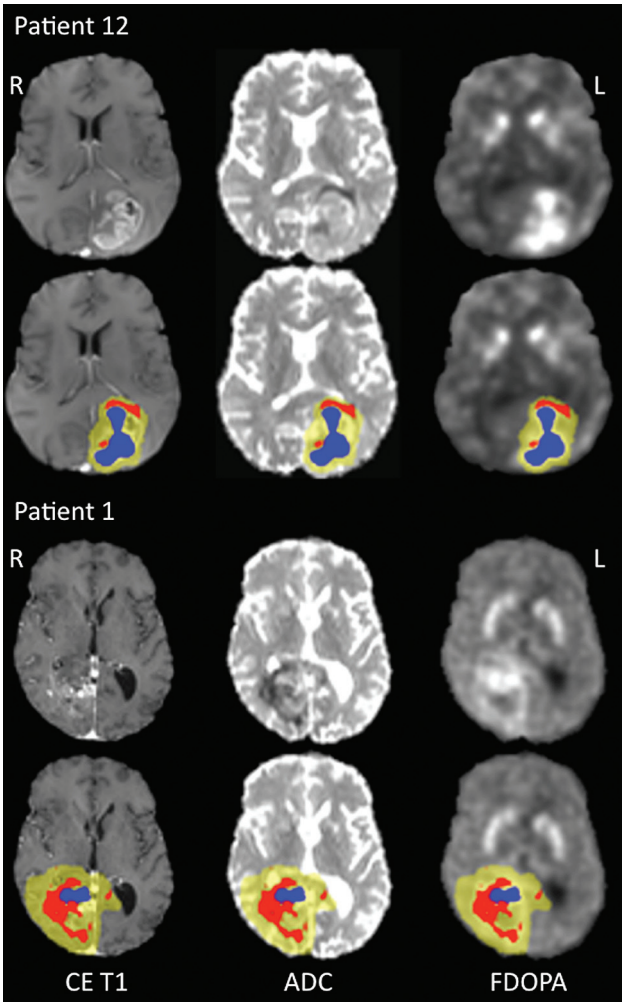

FIG 2. Representative FDOPA–MR imaging fused images for patients 12 (top) and 1 (bottom). The maps from left to right are registered as contrast-enhanced T1-weighted MR imaging, ADC, and FDOPA PET, respectively. For each patient, CE MR imaging, ADC, and FDOPA maps are given without (top) and with overlaid regions of minimum ADC (red), maximum FDOPA SUVR (blue), and FDOPA-defined tumor volume (yellow). All maps are given in radiologic format.

with ADC changing from low to elevated levels with progression of pathology.

To address this problem, Holodny et al[13] investigated the correlation between minimum ADC and FDG uptake in a range of glial tumors and found greater overlap between ADC and FDG compared with gadolinium enhancement on MR imaging. This finding is not surprising because contrast enhancement only delineates blood-brain barrier dysfunction, not tumor infiltration or proliferation. Possible explanations for the correlations found between enhanced FDG metabolism and ADC in some patients were associated with increased cellularity or, potentially, the presence of ischemic tumoral regions. It is known that increased FDG uptake can also reflect increased glycolysis due to focal ischemia.[33] However, significance levels of the correlations were not reported, so it is difficult to judge the robustness of this correlation across the entire patient population in this study.

We found that regions identified with minimum ADC have significantly reduced FDOPA uptake compared with the maximum FDOPA SUVR volume ($P = .0012$), with little or only very modest overlap even when presented as a fraction of the smallest volume, namely the minimum ADC region. The reduced FDOPA SUVR uptake within regions of minimum ADC (1.36 ± 0.22) compared with regions exhibiting maximum FDOPA SUVR uptake (2.45 ± 0.88) may also be explained by the presence of ischemia. At this stage, we do not fully understand all the factors regulating FDOPA uptake within all pathologic tumor regions; however, for the purpose of this study, FDOPA uptake has been shown to significantly correlate with proliferation in newly diagnosed gliomas.[17] As previously outlined, most high-grade gliomas present with elevated ADC within the tumor volume.[28] This observation was consistent in our study. For instance Kang et al[8] reported a mean ADC of $829 \pm 176 \times 10^{-6}$ mm^2/s within the tumor volume in newly diagnosed gliomas by using the same b-value used in our study. The ADC of normal tissue in our study was $530 \pm 29 \times 10^{-6}$ mm^2/s. In this case, the increase in ADC is believed to be associated with edema, early stages of necrosis, liquefaction, and inflammatory processes as a direct result of tumor infiltration.[28] Our finding of elevated FDOPA uptake within these regions (ie, a marker of the presence of metabolically active tumor cells) suggests that such regions could be targets for therapeutic interventions. Clearly, further studies are required to validate such observations.

Another possible explanation for the lack of overlap between regions of minimum ADC and maximum FDOPA SUVR is tissue compression. In an elegant serial study, Lope-Piedrafita et al[32] reported the consistent finding of reduced ADC within the tissue immediately surrounding the growing tumor in an animal glioma model. In this study, histologic analysis indicated that within this region, tissue comprised geometrically asymmetric cells with longer dimensions parallel to the surface of the tumor and the shorter axis normal to the border. It was proposed that the rapid growth in this tumor model exerts pressure on surrounding tissue in a direction normal to the surface of the tumor. This pressure changes the average shape of cells in the immediate vicinity of the tumor from spheric to oblate spheroidal. This compression effect decreased with distance away from the major foci of tumor growth. Such histologic findings would induce a restriction in diffusivity because the compressed cells would effectively have increased cellularity with more membranes per unit volume. Such a concept, if applied in clinical populations, would also help explain the relationship between reduced ADC and poor patient survival, because rapidly expanding (higher grade) tumors are, in many cases, less responsive to treatment. Our finding of minimum overlap between regions of minimum ADC and maximum FDOPA SUVR also supports this mechanism.

Clearly further studies are required to elucidate the pathologic correlates of reduced ADC in GBM. Our findings infer that regions of minimum ADC may primarily be associated with tumor ischemia and/or tissue-compression effects. Where overlap does occur in some patients, minimum ADC most likely infers increased tumor cellularity. Further studies using specific ischemia tracers such as ^{18}F-fluoromisonidazole would help differentiate the effects of ischemia and tissue compression. A measure of tumor perfusion would also help to establish pathologic correlates of minimum ADC. Restricted diffusion has been reported in many studies after successful therapy and is believed to reflect

early efficacious treatment.[34-36] However, in the post-therapy scenario, it is important to note that different pathologic events, induced by the beneficial effects of a chemotherapeutic agent or radiation therapy, will drive cellular mechanisms, resulting in reduced ADC measures. In this study, we focused on investigating restricted diffusion before treatment.

There are a number of limitations with this study: the small number of patients and the lack of histologic data biopsied from regions with minimum ADC. However, acquiring image-guided biopsies before tumor resection is logistically difficult and not normally performed in patients with newly diagnosed high-grade gliomas. For this reason, we have used a PET-based metabolic marker of tumor proliferation. Clearly, additional PET scans using ischemia-specific tracers are also required to fully elucidate the pathologic correlates of restricted diffusivity in GBM. In this study, we used high b-values and a high angular resolution diffusion imaging acquisition protocol to derive ADC measures. This imaging protocol was used to investigate tumor infiltration along white matter pathways by using tractography. Similar to previous reports, our ADC measures were decreased compared with ADC measures derived by using conventional b-values of 1000 s/mm^2 with the diffusion signal dominated by the slow diffusion component.[37] Use of this diffusion parameter would have little impact on our results because a recent study has shown the added value of using high-b-value diffusion imaging for differentiating high- from low-grade gliomas.[8] Most important, within our diffusion image-processing pipeline, we attempted to reduce artifacts induced by physiologic noise and head motion.

CONCLUSIONS

We have shown minimal anatomic correlation between regions exhibiting minimum ADC (a putative marker of tumor cellularity) and maximum FDOPA SUVR uptake (a marker of tumor proliferation). This mismatch supports the concept that restricted diffusion within tumoral regions maybe associated with tissue compression effects and/or possibly the presence of ischemia. Where overlap occurs, enhanced tumor cellularity is most likely to be the major contributing factor. The findings from this study have significant impact on the clinical use of minimum ADC alone as a marker of tumor grade. Combining a metabolic PET proliferation marker with minimum ADC measure may provide a more robust method for guiding tumor biopsies preoperatively.

Disclosures: Stephen Rose—*RELATED*: *Grant*: National Health and Medical Research Council,* *Comments*: I am the principal investigator of a grant that was awarded by the NHMRC to develop novel MRI-PET fusion technology for neuro-oncology applications, *UNRELATED*: *Grants/Grants Pending*: National Health and Medical Research Council.* Michael Fay—*UNRELATED*: *Other*: Abbott Pharmaceuticals Brain Metastases Trial development meeting (London, 2011), transportation to meeting and accommodation only. Paul Thomas—*RELATED*: *Grant*: National Health and Medical Research Council,* *Comments*: The Australian public health research funding body provided the grant for this research. The funding received by our institution was to cover the cost of the imaging performed for this study. *Patents*: Patent Office,* *Comments*: Consideration is being given for an application to patent a method of analyzing PET and MR imaging data for serial comparison. This work was undertaken as part of this research project but is completely unrelated to the work presented in this article. Pierrick Bourgeat—*RELATED*: *Grant*: Queensland Government Smart-State Grant,* *Comments*: grant to develop a new method to help treatment of brain tumors, *UNRELATED*: *Employment:* Commonwealth Scientific and Industrial Research Organization (CSIRO). Nicholas Dowson—*RELATED*: *Grant*: Queensland Smart-State Grant (QSS),* National Health and Medical Research Council,* *Comments*: QSS expired 1 year ago. Olivier Salvado—*RELATED*: *Grant*: QSS,* National Health and Medical Research Council,* *Comments*: QSS expired 1 year ago, *UNRELATED*: *Other*: GE Healthcare,* *Comments*: involved in a contract with GE Healthcare unrelated to this work. Yaniv Gal—*RELATED*: *Grant*: National Health and Medical Research Council (Australia), *Comments*: The NHMRC grant money is paying my salary. Stuart Crozier—*RELATED: Grant*: National Health and Medical Research Council federal project grant,* *Comments*: Standard National Institutes of Health–equivalent grant, *UNRELATED*: *Grants/Grants Pending*: National Health and Medical Research Council grant.* *Money paid to the institution.

REFERENCES

1. DeAngelis LM. **Brain tumors.** *N Engl J Med* 2001;344:114–23
2. Johnson PC, Hunt SJ, Drayer BP. **Human cerebral gliomas: correlation of postmortem MR imaging and neuropathologic findings.** *Radiology* 1989;170:211–17
3. Jacobs AH, Thomas A, Kracht LW, et al. **^{18}F-fluorothymidine and ^{11}C-methymethionine as markers of increased transport and proliferation in brain tumors.** *J Nucl Med* 2005;46:1948–58
4. Chen W, Silverman DH, Delaloye S, et al. **^{18}F-FDOPA PET imaging of brain tumors: comparison study with ^{18}F-FDG PET and evaluation of diagnostic accuracy.** *J Nucl Med* 2006;47:904–11
5. Ledezma CJ, Chen W, Sai V, et al. **^{18}F-FDOPA PET/MRI fusion in patients with primary/recurrent gliomas: initial experience.** *Eur J Radiol* 2009;71:242–48
6. Kim S, Chung JK, Im SH, et al. **11C-methionine PET as a prognostic marker in patients with glioma: comparison with 18F-FDG PET.** *Eur J Nucl Med Mol Imaging* 2005;32:52–59
7. Cha S. **Update on brain tumor imaging: from anatomy to physiology.** *AJNR Am J Neuroradiol* 2006;27:475–87
8. Kang Y, Choi SH, Kim YJ, et al. **Gliomas: histogram analysis of apparent diffusion coefficient maps with standard- or high-*b*-value diffusion-weighted MR imaging: correlation with tumor grade.** *Radiology* 2011;261:882–90
9. Murakami R, Hiarir T, Sugahara T, et al. **Grading astrocytic tumors by using apparent diffusion coefficient parameters: superiority of a one- versus two-parameter pilot method.** *Radiology* 2009;251:838–45
10. Zonari P, Baraldi P, Crisi G, et al. **Multimodal MRI in the characterization of glial neoplasms: the combined role of single-voxel MR spectroscopy, diffusion imaging and echo-planer perfusion imaging.** *Neuroradiology* 2007;49:795–803
11. Catalaa I, Henry R, Dillion WP, et al. **Perfusion, diffusion and spectroscopy values in newly diagnosed cerebral gliomas.** *NMR Biomed* 2006;19:463–75
12. Higano S, Yun X, Kumabe T, et al. **Malignant astrocytic tumors: clinical importance of apparent diffusion coefficient in prediction of grade and prognosis.** *Radiology* 2006;241:839–46
13. Holodny AI, Makeyev S, Beattie BJ, et al. **Apparent diffusion coefficient of glial neoplasms: correlation with fluorodeoxyglucose-position-emission tomography and gadolinium-enhanced MR imaging.** *AJNR Am J Neuroradiol* 2010;31:1042–48
14. Ricci PE, Karis JP, Heiserman JE, et al. **Differentiating recurrent tumor from radiation necrosis: time for re-evaluation of position emission tomography.** *AJNR Am J Neuroradiol* 1998;19:407–13
15. Becherer A, Karanikas G, Szabo M, et al. **Brain tumor imaging with PET: a comparison between [18F]fluorodopa and [11C]methionine.** *Eur J Nucl Med Mol Imaging* 2003;30:1561–67
16. Schiepers C, Chen W, Cloughesy T, et al. **18F-FDOPA kinetics in brain tumors.** *J Nucl Med* 2007;48:1651–61
17. Fueger BJ, Czernin J, Cloughesy T, et al. **Correlation of 6–18F-fluoro-L-dopa PET with proliferation and tumor grade on newly diagnosed and recurrent gliomas.** *J Nucl Med* 2010;51:1532–38
18. Namavari M, Bishop A, Satyamurthy N, et al. **Regioselective radiofluorodestannylation with [18F]F2 and [18F]Ch3COOF: a high yield synthesis of 6-[^{18}F]fluoro-L-dopa.** *Int J Rad Appl Instrum A* 1992;43:989–96
19. Nuyts J, Michel C, Dupont P. **Maximum-likelihood expectation-maximization reconstruction of sinograms with arbitrary noise distribution using NEC-transformations.** *IEEE Trans Med Imaging* 2001;20:365–75

20. Kinahan PE, Townsend DW, Beyer T, et al. **Attenuation correction for a combined 3D PET/CT scanner.** *Med Phys* 1998;25:2046–53
21. Rose SE, Pannek K, Bell C, et al. **Direct evidence of intra- and interhemispheric corticomotor network degeneration in amyotrophic lateral sclerosis: an automated MRI structural connectivity study.** *Neuroimage* 2012;59:2661–69
22. Bai Y, Alexander DC. **Model-based registration to correct for motion between acquisitions in diffusion MR imaging.** In: *IEEE International Symposium on Biomedical Imaging: From Nano to Macro,* London, UK. 2008;1–4:947–50
23. Rohde GK, Barnett AS, Basser PJ, et al. **Comprehensive approach for correction of motion and distortion in diffusion-weighted MRI.** *Magn Reson Med* 2004;51:103–14
24. Morris D, Nossin-Manor R, Taylor MJ, et al. **Preterm neonatal diffusion processing using detection and replacement of outliers prior to resampling.** *Magn Reson Med* 2011;66:92–101
25. Tournier JD, Calamante F, Connelly A. **Robust determination of the fiber orientation distribution in diffusion MRI: non-negativity constrained super-resolved spherical deconvolution.** *Neuroimage* 2007;35:1459–72
26. Ourselin S, Roche A, Subsol G, et al. **Reconstructing a 3D structure from serial histological sections.** *Image and Vision Computing* 2001;19:25–31
27. Vees H, Senthamizhchelvan S, Miralbell R, et al. **Assessment of various strategies for 18F-FET PET-guided delineation of target volumes in high-grade glioma patients.** *Eur J Nucl Med Mol Imaging* 2009;36:182–93
28. Hakyemez B, Erdogan C, Yildirim N, et al. **Glioblastoma multiforme with atypical diffusion-weighted MR findings.** *Br J Radiol* 2005;78:989–92
29. Stadnik TW, Chaskis C, Mihotte A, et al. **Diffusion-weighted MR imaging of intracerebral masses: comparison with conventional MR imaging and histological findings.** *AJNR Am J Neuroradiol* 2001;22:969–76
30. Mills SJ, Soh C, Rose CJ, et al. **Candidate biomarkers of extravascular extracellular space: q direct comparison of apparent diffusion coefficient and dynamic contrast-enhanced MRI imaging—derived measurement of the volume of the extravascular extracellular space in glioblastoma multiforme.** *AJNR Am J Neuroradiol* 2010;31:549–53
31. Baehring JM, Bi WL, Bannykh S, et al. **Diffusion MRI in the early diagnosis of malignant glioma.** *J Neurooncol* 2007;82:221–25
32. Lope-Piedrafita S, Garcia-Martin ML, Galons JP, et al. **Longitudinal diffusion tensor imaging in a rat brain glioma model.** *NMR Biomed* 2008;21:799–808
33. Rajendran JG, Mankoff DA, O'Sullivan F, et al. **Hypoxia and glucose metabolism in malignant tumors: evaluation by [18F]fluoromisonidazole and [18F]fluorodeoxyglucose positron emission tomography imaging.** *Clin Cancer Res* 2004;10:2245–52
34. Gupta A, Young RJ, Karimi S, et al. **Isolated diffusion restriction preceded the development of enhancing tumor in a subset of patients with glioblastoma.** *AJNR Am J Neuroradiol* 2011;32:1301–06
35. Ellingson BM, Cloughesy TF, Lai A, et al. **Graded functional diffusion map-defined characteristics of apparent diffusion coefficients predict overall survival in recurrent glioblastoma treated with bevacizumab.** *Neuro Oncol* 2011;13:1151–61
36. Moffat BA, Chenevert TL, Lawrence TS, et al. **Functional diffusion map: a noninvasive MRI biomarker for early stratification of clinical brain tumor response.** *Proc Natl Acad Sci U S A* 2005;102:5524–29
37. DeLano MC, Cooper TG, Siebert JE, et al. **High-b-value diffusion-weighted MR imaging of adult brain: image contrast and apparent diffusion coefficient map features.** *AJNR Am J Neuroradiol* 2000;21:1830–36